Supporting Information

Revisiting the quasi-aromaticity in polynuclear metal chalcogenide clusters and its derivative "cluster-assembly" crystalline structures

Bochu Wang[1,2] and Wan-Lu Li*[1,3]

[1]Department of NanoEngineering, University of California San Diego, CA 92093
[2]Department of Chemistry, University of California San Diego, CA 92093
[3]Program of Materials Science and Engineering, University of California San Diego, CA 92093
*Corresponding Author: wal019@ucsd.edu

Table S1. Optimized bond parameters of $[M_3X_4(H_2O)_9]^{4+}$ clusters (M = Cr, Mo, W, Sg; X = O, S, Se, Te) at SR-ZORA PBE/VTZ level, and the single (r_1) and double (r_2) M–M bonds based on the latest recommended covalent radii by Pyykkö, which are all in Å.

	M–M	X^b–X^b	M–X^c	M–X^b	r_1(M–X)	r_2(M–X)	M–H_2O
$[Cr_3O_4(H_2O)_9]^{4+}$	2.394	2.640	1.901	1.775	1.85	1.68	2.106 (2.090)[a]
$[Mo_3O_4(H_2O)_9]^{4+}$	2.552	2.834	2.068	1.919	2.01	1.78	2.237 (2.221)
$[W_3O_4(H_2O)_9]^{4+}$	2.543	2.845	2.081	1.925	2.00	1.77	2.226 (2.207)
$[Sg_3O_4(H_2O)_9]^{4+}$	2.648	2.939	2.176	1.999	2.06	1.85	2.302 (2.271)
$[Cr_3S_4(H_2O)_9]^{4+}$	2.708	3.178	2.233	2.164	2.25	2.05	2.171 (2.151)
$[Mo_3S_4(H_2O)_9]^{4+}$	2.791	3.404	2.374	2.294	2.41	2.15	2.291 (2.279)
$[W_3S_4(H_2O)_9]^{4+}$	2.766	3.465	2.394	2.314	2.40	2.14	2.273 (2.262)
$[Sg_3S_4(H_2O)_9]^{4+}$	2.884	3.606	2.509	2.409	2.46	2.22	2.339 (2.325)
$[Cr_3Se_4(H_2O)_9]^{4+}$	2.830	3.349	2.370	2.304	2.38	2.18	2.183 (2.168)
$[Mo_3Se_4(H_2O)_9]^{4+}$	2.850	3.597	2.497	2.424	2.54	2.28	2.308 (2.295)
$[W_3Se_4(H_2O)_9]^{4+}$	2.792	3.640	2.511	2.434	2.53	2.27	2.288 (2.280)
$[Sg_3Se_4(H_2O)_9]^{4+}$	2.858	3.761	2.595	2.505	2.59	2.35	2.354 (2.347)
$[Cr_3Te_4(H_2O)_9]^{4+}$	3.000	3.683	2.581	2.520	2.58	2.39	2.192 (2.172)
$[Mo_3Te_4(H_2O)_9]^{4+}$	2.938	3.905	2.699	2.633	2.74	2.49	2.332 (2.323)
$[W_3Te_4(H_2O)_9]^{4+}$	2.842	3.961	2.720	2.646	2.73	2.48	2.315 (2.313)
$[Sg_3Te_4(H_2O)_9]^{4+}$	2.888	4.087	2.805	2.716	2.79	2.56	2.385 (2.380)

[a] Results without parentheses are corresponding to the distances between M and the H_2O moiety near X^c; results in the parentheses are the distances between M and the H_2O near X^b atoms.

Table S2. Orbital types transformed irreducible representations and the corresponding bonding types of d-based AOs in M_3 cluster with C_{3v} symmetry.

Orbital type	Irreducible representation	Bonding type
Γd_z^2	a_1	σ_r
	e	σ_r^*
Γd_{xz}	e	σ_t
	a_2	σ_t^*
Γd_{yz}	a_1	π_r
	e	π_r^*
Γd_{xy}	e	π_t
	a_2	π_t^*
$\Gamma d_{x^2-y^2}$	a_1	δ_v
	e	δ_v^*

Table S3. M–M, X^b–X^b and M–X^b bond orders indices of $[M_3X_4(H_2O)_9]^{4+}$ clusters (M = Cr, Mo, W, Sg; X = O, S, Se, Te) at PBE/VTZ level.

BO		X = O				X = S				X = Se				X = Te			
		Cr	Mo	W	Sg	Cr	Mo	W	Sg	Cr	Mo	W	Sg	Cr	Mo	W	Sg
Mayer	M–M	0.73	0.74	0.92	1.11	0.76	0.77	0.90	0.94	0.70	0.71	0.79	0.87	0.82	0.85	0.86	1.02
	X^b–X^b	0.02	0.04	0.03	0.03	0.04	0.03	0.03	0.04	0.04	0.01	0.02	0.04	0.05	0.03	0.04	0.05
	M–X^b	1.02	0.91	0.90	0.89	1.31	1.24	1.23	1.20	1.31	1.22	1.22	1.22	1.50	1.46	1.45	1.43
G-J	M–M	0.69	0.76	0.81	0.85	0.64	0.67	0.74	0.79	0.65	0.68	0.75	0.80	0.66	0.69	0.77	0.84
	X^b–X^b	0.04	0.05	0.05	0.04	0.06	0.06	0.05	0.05	0.07	0.06	0.06	0.06	0.09	0.07	0.06	0.06
	M–X^b	1.04	1.00	0.97	0.95	1.17	1.15	1.13	1.11	1.17	1.16	1.13	1.11	1.19	1.17	1.16	1.13
N-M(1)	M–M	0.79	0.86	0.97	1.00	0.71	0.74	0.85	0.89	0.72	0.75	0.86	0.90	0.73	0.75	0.87	0.92
	X^b–X^b	0.05	0.06	0.05	0.05	0.05	0.06	0.06	0.06	0.07	0.06	0.06	0.06	0.09	0.07	0.06	0.07
	M–X^b	1.15	1.12	1.14	1.12	1.24	1.24	1.23	1.21	1.24	1.23	1.21	1.20	1.25	1.24	1.22	1.20
N-M(3)	M–M	0.64	0.69	0.77	0.79	0.63	0.66	0.75	0.77	0.65	0.67	0.76	0.79	0.67	0.70	0.80	0.83
	X^b–X^b	0.05	0.06	0.06	0.06	0.06	0.06	0.06	0.06	0.07	0.06	0.06	0.06	0.08	0.06	0.06	0.06
	M–X^b	1.12	1.11	1.10	1.09	1.17	1.15	1.15	1.14	1.16	1.15	1.14	1.13	1.15	1.14	1.12	1.11

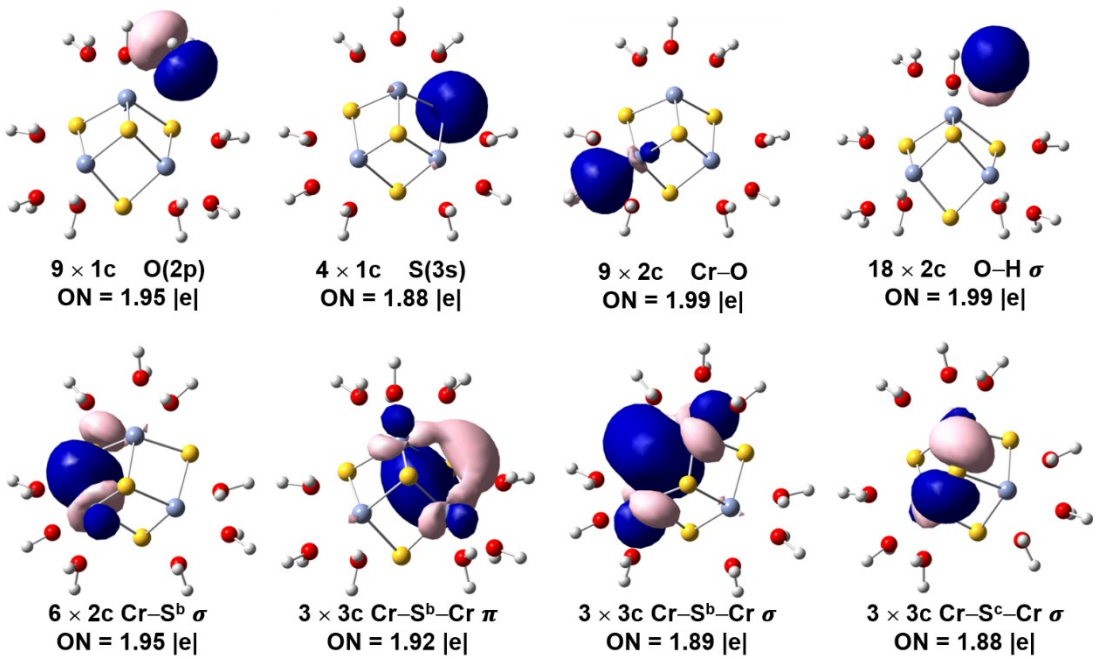

Figure S1. AdNDP localized orbitals of $[Cr_3S_4(H_2O)_9]^{4+}$ at the PBE/VTZ level. ON means the occupation number (isosurface value = 0.02 au).

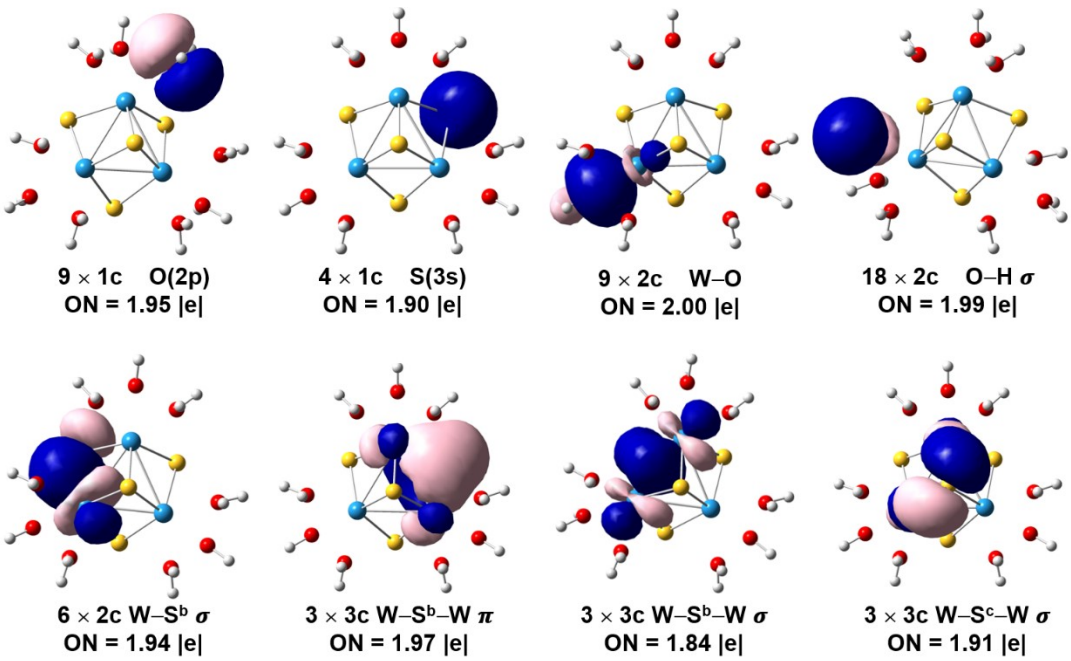

Figure S2. AdNDP localized orbitals of $[W_3S_4(H_2O)_9]^{4+}$ at the PBE/VTZ level. ON means the occupation number (isosurface value = 0.02 au).

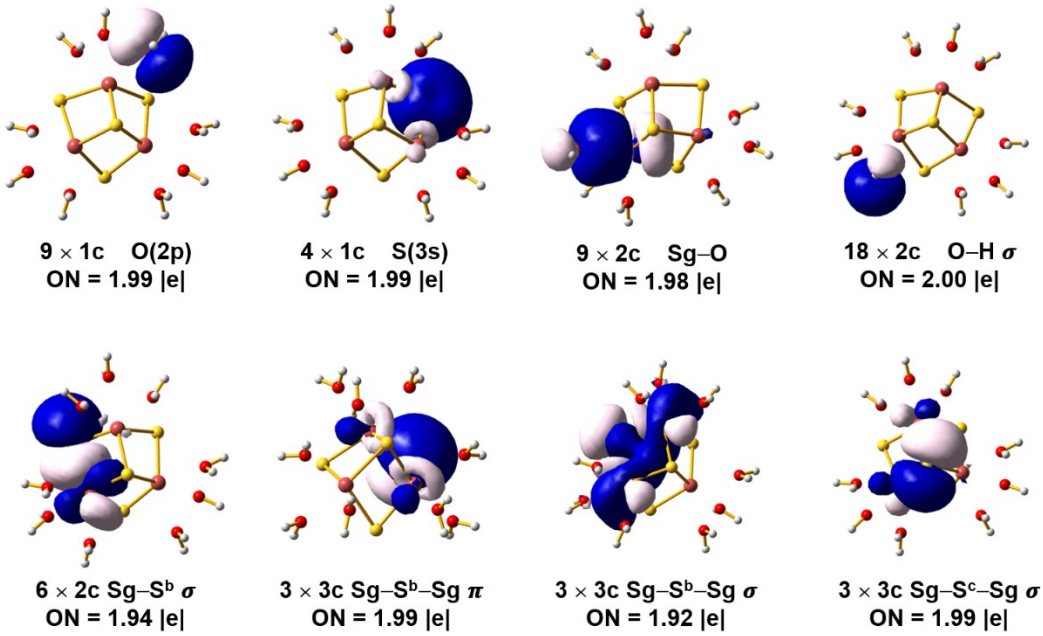

Figure S3. AdNDP localized orbitals of $[Sg_3S_4(H_2O)_9]^{4+}$ at the PBE/VTZ level. ON means the occupation number (isosurface value = 0.02 au).

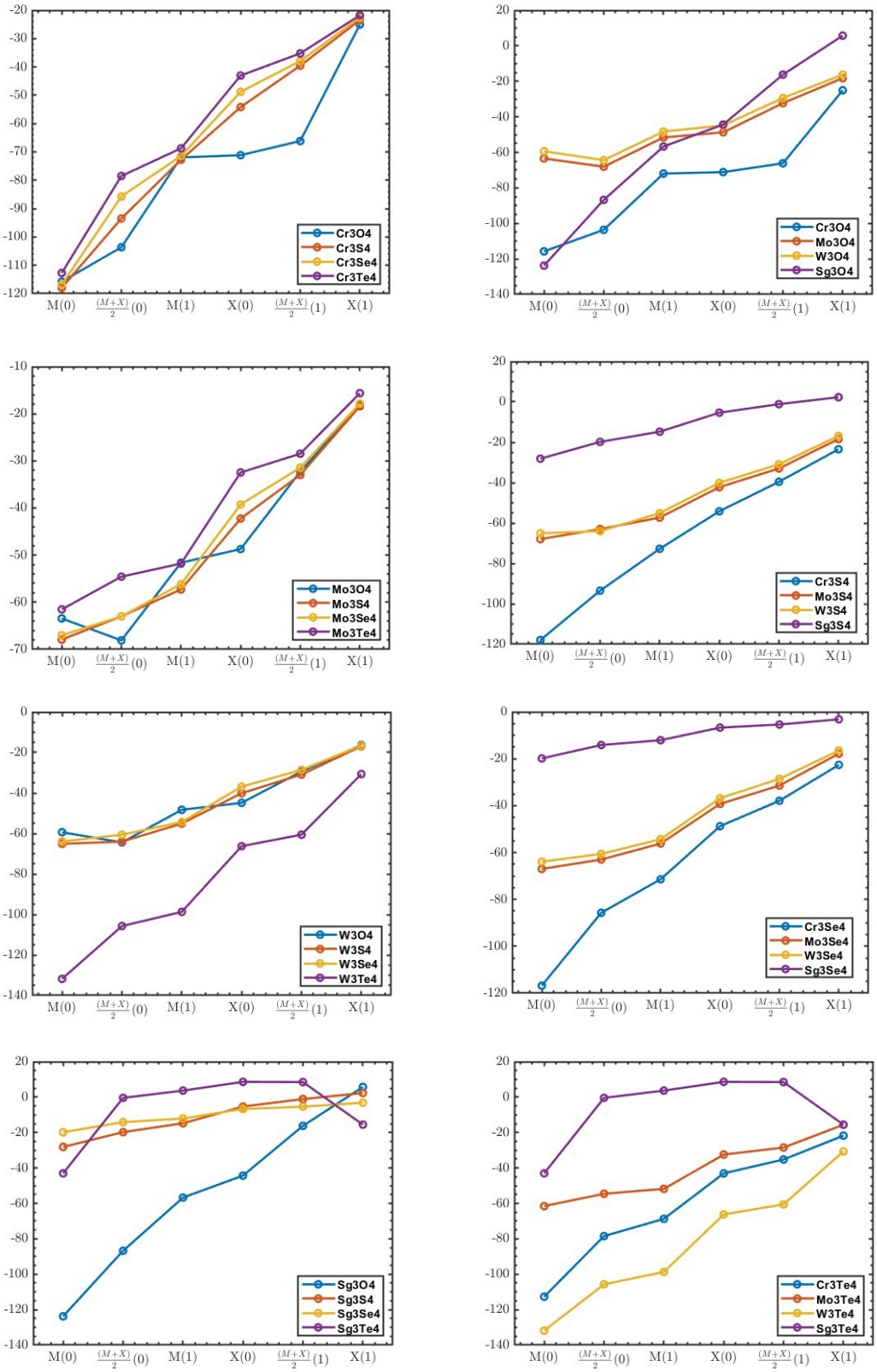

Figure S4. The NICS values of all 16 $[M_3X_4]^{4+}$ clusters (a: M = Cr, Mo, W, Sg; b: X = O, S, Se, Te) at PBE/VTZ level. The NICS values of Sg_3Te_4 were calculated at B3LYP level.

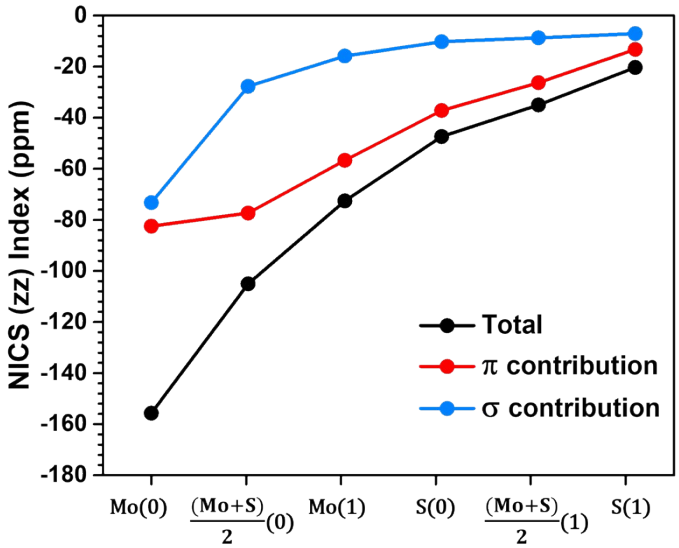

Figure S5. The $NICS_{zz}$ values of $[Mo_3S_4]^{4+}$ at B3LYP/VTZ level, as well as the contributions from the σ and π components. Six special points are considered: centers of Mo_3 plane Mo (0), S_3 plane S (0), half between Mo_3 and S_3 plane $\frac{(Mo+S)}{2}$ (0), and 1 Å above each plane: Mo (1), S (1) and $\frac{(Mo+S)}{2}$ (1).

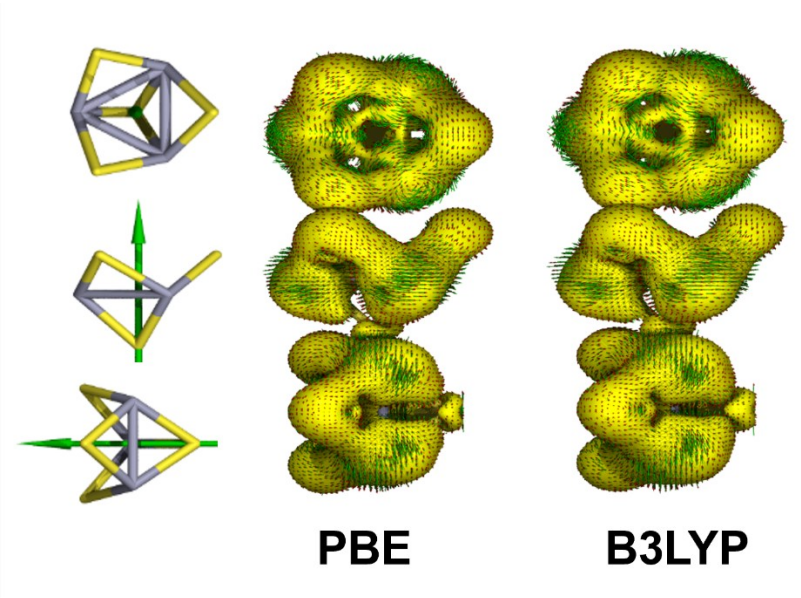

Figure S6. The MICD current diagrams of $Mo_3S_4^{4+}$ from three different views at the levels of PBE and B3LYP functionals with VTZ basis sets. The red and green color in the contour plot correspond to the arrowhead and tail, respectively.

Table S4. Energy integral (–ICOHP, in eV/bond) values and electronic states in $BaMo_6S_8$, and atomic charges in *e* as obtained from Mulliken (M) and Löwdin (L) population approaches.

–ICOHP		Electronic configuration and valence charge					
		Mo		S		Ba	
Mo–S	Mo–Mo	M ($4d^{5.14}5s^{0.52}$)[a]	L ($4d^{5.23}5s^{0.51}$)	M ($3s^{1.78}3p^{4.67}$)	L ($3s^{1.64}3p^{4.63}$)	M ($6s^{0.26}3p^{0.30}$)	L ($6s^{0.44}3p^{1.11}$)
-2.53	-1.65	0.34 (0.24)[b]	0.26	-0.45 (-0.43)	-0.27	1.49	0.55

[a] Values in the parentheses in this raw correspond to the electronic structures from Mulliken (M) and Löwdin (L) methods.
[b] Values in the parentheses in this raw correspond to the Mulliken charge on Mo and S atoms in $Mo_6S_8^{2-}$ cluster for comparison.

Table S5. Bader atomic charges in *e* of Mo_3S_6 cluster for comparison with MoS_2 nanomaterial.

	Mo	S
Mo_3S_6 cluster	0.99	-0.50
MoS_2 nanomaterial	0.88	-0.44

Table S6. Geometric parameter (length in Å and angle in °) comparison of theoretical Mo_3S_4 nanomaterials and Mo_6S_8 cluster at GGA/PBE level.

	a	*b*	*c*	*α*	*β*	*γ*	Mo–S[a]	Mo–Mo[a]
Theo. $BaMo_6S_8$	9.29	9.29	9.29	90.00	90.00	120.0	2.4388	2.8363
$Mo_6S_8^{2-}$	-	-	-	-	-	-	2.4364	2.6277

[a] The bond lengths of Mo–S and Mo–Mo are the average values in both Mo_3S_4 nanomaterials and Mo_6S_8 cluster.

Table S7. Bader atomic charges in *e* of Mo_6S_8 cluster for comparison with Mo_3S_4 nanomaterial.

	Mo	S
Mo_6S_8 cluster	0.79	-0.59
Mo_3S_4 nanomaterial	0.76	-0.57

Table S8. Orbital types transformed irreducible representations of d-based AOs in octahedral clusters.

Orbital type	Irreducible representation
Γd_{xy}	$a_{2u} + e_u + t_{2g}$
$\Gamma d_{x^2-y^2}$	$a_{2g} + e_g + t_{2u}$
Γd_{z^2}	$a_{1g} + e_g + t_{1u}$
$\Gamma(d_{xz}, d_{yz})$	$t_{1g} + t_{2g} + t_{1u} + t_{2u}$

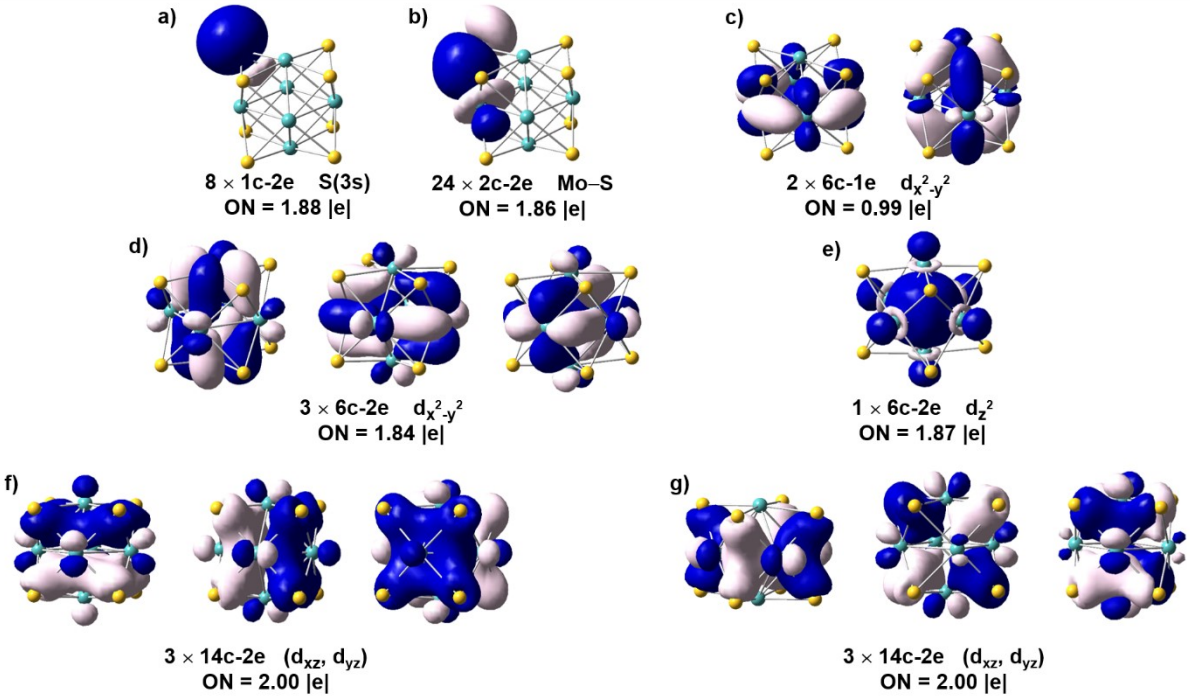

Figure S7. Localized orbitals of $Mo_6S_8^{2-}$ revealed by AdNDP methods at the PBE/VTZ level.